Analysis Note for $\gamma p \to p\phi\eta$

Bradford E. Cannon

January 23, 2018

Table of Contents

1 Analysis of $\gamma p \to p\phi\eta$

In order to study potential states of bound strangeonia, it is essential to properly identify all final and initial state particles. The final state topology that will be studied for this thesis is $\gamma p \to pK^+K^-\gamma_1\gamma_2$, where the K^+K^- pair are daughter states of the ϕ meson, and the $\gamma_1\gamma_2$ pair are daughter states of the η meson. Therefore, the beginning of this analysis section will focus on the particle identification of the proton, kaons, and final state photons, as well as the incident beam and target proton. Once identification of all particles has been well established, this analysis will then investigate whether or not a correlation exists between the ϕ and η bound states. This analysis will be conducted by means of sampling different regions of the $\gamma_1\gamma_2$ invariant

mass and the K^+K^- invariant mass. Ultimately, it will be shown that a correlation does in fact manifest itself within this data set, and therefore a thorough strangeonia analysis can be performed.

1.1 Spring 2017 Run Period

The data presented here is the result of the successful the Spring 2017 Low Intensity run period. The Spring 2017 run period spanned from January 23rd to March 13th and accumulated roughly 50 billion physics events. The maximum electron beam energy used was 12 GeV, and the accelerator ran at 250 MHz while in low intensity (beam every 4 ns), and later ran at 500 MHz while in high intensity. Upon entering Hall D, the electron beam was incident upon a radiator. During this run period, both amorphous and diamond radiators were used to produce either incoherent or coherent polarized bremsstrahlung radiation. The diamond radiator was experimentally set up to produce linear photon polarization at four different angles; 0°, 45°, 90°, and 135°. These directions were chosen in order to provide the detector with a uniform sampling of linear polarization. In order to yield roughly the same amount of statistics for an amorphous radiator run as compared to a diamond radiator run, a beam current of 150 nA was incident upon the amorphous radiator, while a beam current of 100 nA was incident upon the diamond radiator. Farther downstream, a 5mm collimator hole was used for all radiator configurations. Lastly, the collimated photon beam was incident upon a stationary liquid hydrogen target. This resulted in one petabyte of files and $16pb^{-1}$ of integrated luminosity.

1.2 Particle Identification

Once all of the data files were written to disk, an analysis launch was initiated. Part of this analysis launch searched for the $\gamma p \to pK^+K^-\gamma\gamma$ topology and incorporated a kinematic fitter which simultaneously constrained four momentum and a common production vertex for the final state particles. It should be noted that this analysis did not enforce the K^+K^- pair come from a ϕ parent state, or the $\gamma\gamma$ pair come from an η parent state; even though the ultimate goal of this analysis is to study the parent states of $\phi\eta$. After successful completion of the analysis launch, the data was then processed by a DSelector which applied several cuts to the data. Initial cuts on the data included timing cuts in the Barrel Calorimeter (BCAL), Forward Calorimeter (FCAL), and the Time of Flight detector (TOF). These timing cuts were made for all of the final state particles $(p, K^+, K^-, \gamma_1, \gamma_2)$. A table of the timing cuts used for each final state particle and its associated

detector apparatus is given in Table 1. A list of timing plots for all of the final state particles and detector systems is given in Figures 1234. In these Figures, the left plots include timing measurements from the BCAL, the middle plots include timing measurements from the FCAL, and the right plot includes timing measurements from the TOF. All plots have the timing on the vertical axis and the measured magnitude of the three momentum on the horizontal axis. The 'z' axis is logarithmically scaled with the relative values given by the color bar to the of the plots. The ΔT measurement comes from comparing the measured timing from the associated detector with the time reported by the RF, or beam. To identify particles, we want to only select candidates that have a ΔT close to zero.

Particle	Detector	ΔT Cut [ns]
Proton	BCAL	$\pm$ 0.40
Proton	FCAL	$\pm$ 1.00
Proton	TOF	$\pm$ 0.30
K^+	BCAL	$\pm$ 0.40
K^+	FCAL	$\pm$ 0.50
K^+	TOF	$\pm$ 0.20
K^-	BCAL	$\pm$ 0.40
K^-	FCAL	$\pm$ 0.50
K^-	TOF	$\pm$ 0.20
γ	BCAL	$\pm$ 0.50
γ	FCAL	$\pm$ 0.75

Table 1: A table with timing cut values for all final state particles in the reaction $\gamma p \to pK^+K^-\gamma_1\gamma_2$. The values of the timing cuts change depending on both the particle species and detector system resolution. It should be noted that the final state photons only have the calorimeters as possible timing detectors. This is due to the fact that they do not interact with the TOF detector.

After the timing cuts for all of the final state particles was performed, additional cuts were made to identify the $\gamma p \to pK^+K^-\gamma_1\gamma_2$ final state. One of these cuts included enforcing the reconstructed vertex for all final state particles to be within the geometric volume of the target chamber. Since this analysis does not contain a particle lifetime which would result in a detached vertex, it is imperative to remove backgrounds from other channels that may have this feature, such as excited baryons with a strange quark. An example of what the reconstructed vertex for the final state photons looks like in the z direction (along the beam direction) and in the x-y plane (transverse to the

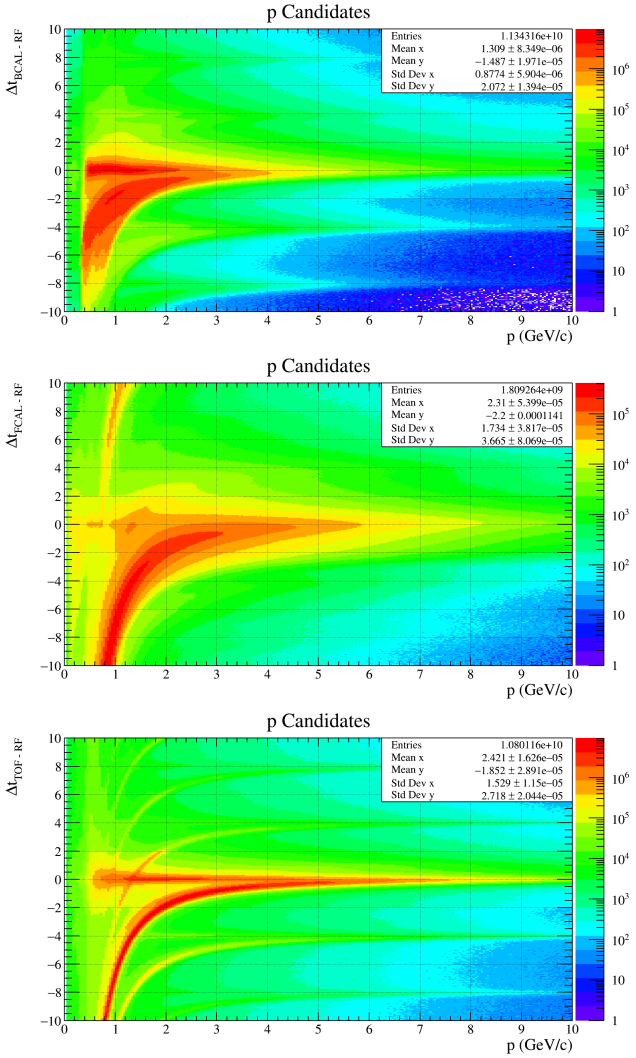

Figure 1: Timing plots for proton candidates at GlueX. Protons are identified by selecting the horizontal band centered about $\Delta T = 0$. The curved line deviating below the horizontal proton line comes from miss identified π^+ tracks. The additional curved lines above and below $\Delta T = 0$ come from π^+ tracks that are associated with the wrong RF bunch.

beam direction), as well as the associated cut values, is given in Figure 5.

Another additional cut that is made on the data pertains directly to the identification of the correct beam photon bunch. Since the electron beam is delivered from the accelerator every four nanoseconds, the timing of when the particles arrive into the hall is well known and we call the the Radio Frequency (RF) time. However, once the photons are in the hall, it is unclear

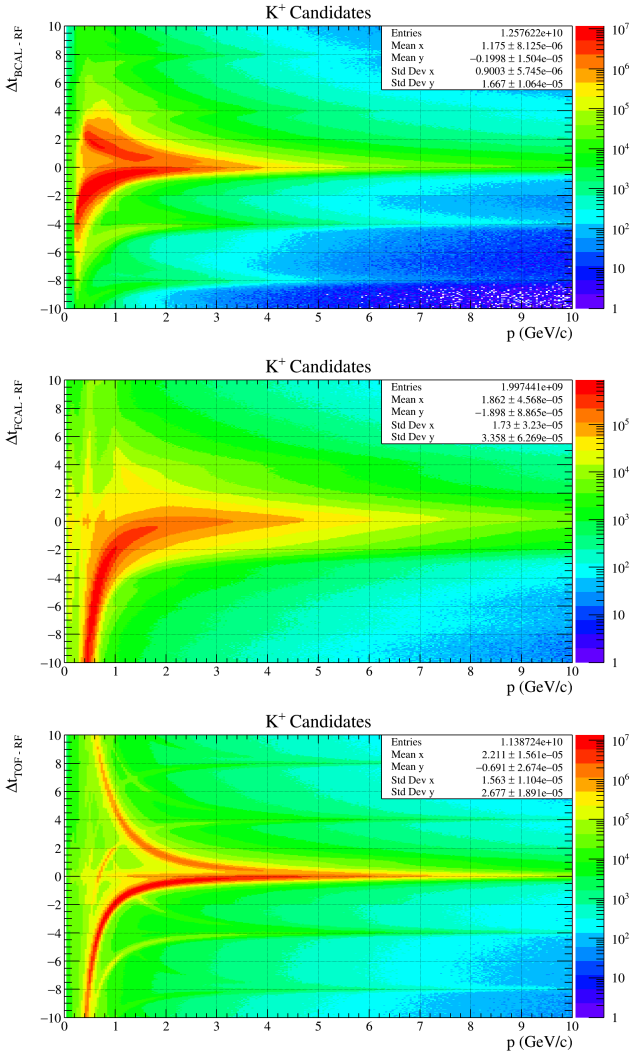

Figure 2: Timing plots for K^+ candidates at GlueX. K^+ are identified by selecting the horizontal band centered about $\Delta T = 0$. The curved line deviating below the horizontal K^+ line comes from miss identified π^+ tracks, and the curved line deviating above the horizontal K^+ line comes from miss identified proton tracks. The additional curved lines above and below $\Delta T = 0$ come from π^+ and proton tracks that are associated with the wrong RF bunch.

which beam bunch may have caused the subsequent physics event. When a physics event takes place, there is an associated beam time which is recoded by either the tagger hodoscope or the tagger microscope. This device can measure both the energy of the beam and the timing of the beam. One of the

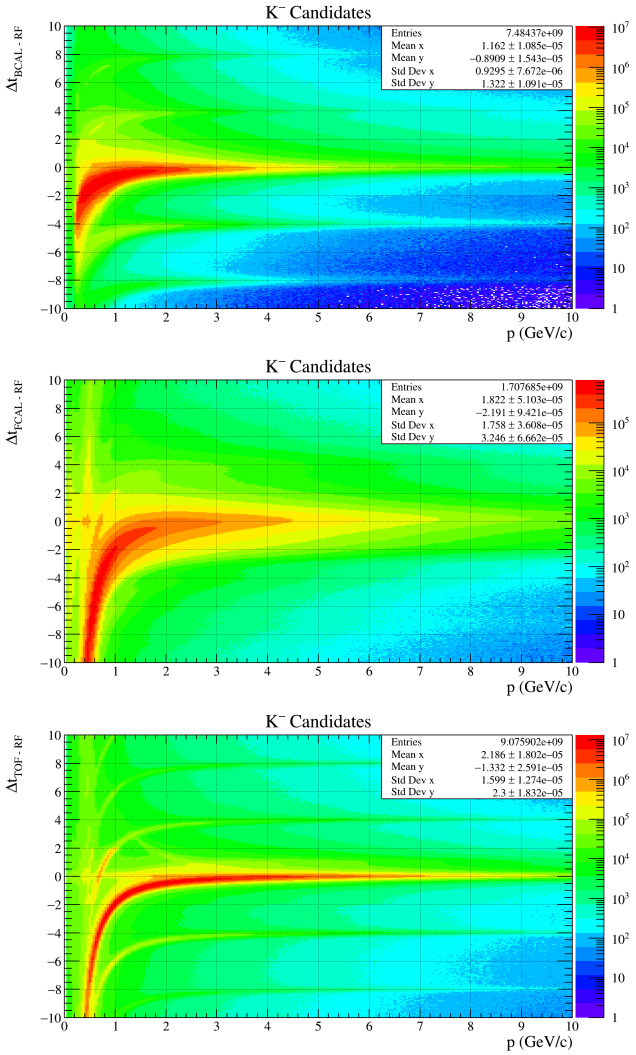

Figure 3: Timing plots for K^- candidates at GlueX. K^- are identified by selecting the horizontal band centered about $\Delta T = 0$. The curved line deviating below the horizontal K^- line comes from miss identified π^- tracks. The additional curved lines above and below $\Delta T = 0$ come from π^- tracks that are associated with the wrong RF bunch.

cuts is made on the the data presented is the difference between the recorded beam time and the reported RF time. An example of what this data looks like and the cut used for it is given in Figure 6.

The last cut that was performed by the DSelector was the value of the observed beam energy. Although this cut does not technically fall under the category of a particle identification, it is included in this section because it

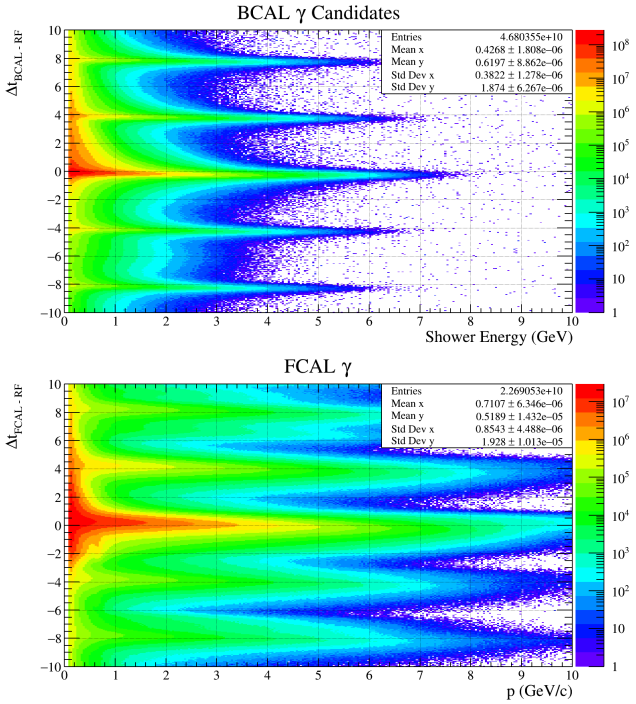

Figure 4: Timing plots for γ candidates at GlueX. γ are identified by selecting the horizontal band centered about $\Delta T = 0$. Large enhancement in statistics at low momentum and out of time with the γ line comes from slow moving and poorly times neutrons. The additional horizontal lines above and below $\Delta T = 0$ come from γ showers that are associated with the wrong RF bunch.

was used as a prerequisite for the rest of this analysis. Since this study will ultimately focus on a reaction which requires a high 't' momentum transfer, it is natural to only allow beam photons with high momentum to begin with. This, coupled with the fact that low energy photons produce low statistics for this channel, is the reason why a beam energy cut of $Beam_E \geq 7.5$ GeV was enforced early in the analysis. It should also be noted that this analysis will include a beam asymmetry study for strangeonia which will force the beam energy to be within the coherent peak region $(8.0GeV - 8.8GeV)$. An example beam energy distribution with the associated cut is given in Figure 7.

1.3 Kinematic Fit Confidence Level Cut Study

This is where I am... Need to continue editing document from here...The first of the cuts included a kinematic fit confidence level cut of $1x10^{-4}$. This

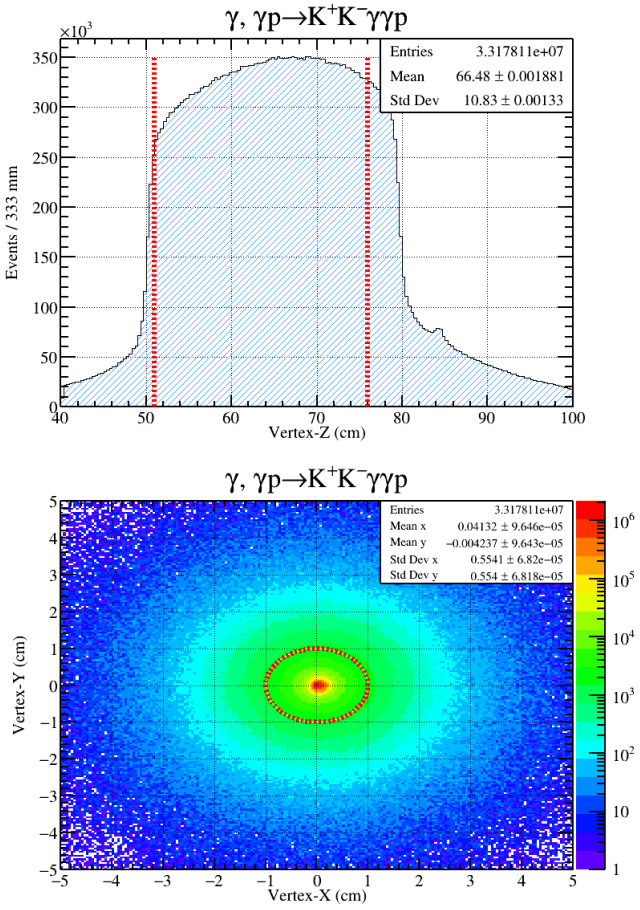

Figure 5: An example of what a reconstructed vertex distribution looks like for a final state γ in the reaction $\gamma p \to pK^+K^-\gamma_1\gamma_2$. The upper image is the reconstructed vertex position along the beam line, or z axis; and the lower image is the reconstructed vertex position in the directions transverse to the beam line. Both figures contain red dashed lines which represent the cut values for all reconstructed final state particles. In the z direction the cut values are $51cm \leq V_z \leq 76cm$, and in the transverse direction the cut values are $V_r \leq 1cm$.

kinematic fit confidence level was chosen based on a study that was performed on this data after it was processed by the analysis launch. In this study, both the η and ϕ peaks from the $\gamma\gamma$ and K^+K^- invariant mass spectra were fitted as a function of kinematic fit confidence level cut. The η peak was fitted with a Gaussian plus a first degree polynomial while the ϕ peak was fitted with a Gaussian plus a second degree polynomial. Examples of an η fit from this study is given in Figure 8, and an example ϕ fit from this study is given in

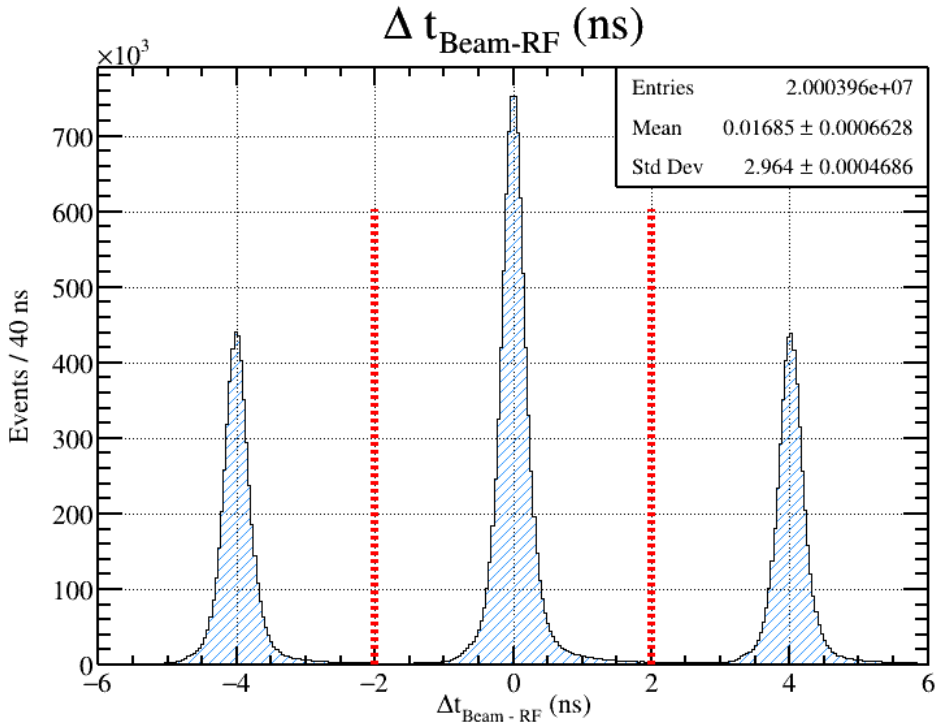

Figure 6: An example histogram of beam time as compared to the reported Radio Frequency (RF) time. In the plot there are three peaks, all of which are separated by four nanoseconds. Also included in the plot are two red dashed cut lines at ±2 ns. These cut lines will select the beam time which agrees with the RF and will reject the other out of time beam particles.

Figure 9. In each figure, the blue line represents the sum of the Gaussian plus the polynomial fits, the green line represents the Gaussian fit, and the red line represents the polynomial fit. Additionally, both figures are the result of a kinematic fit confidence level cut of $1x10^{-4}$. It should be noted that the mean values and widths obtained from these Gaussian fits will serve as the observed massed and widths for the rest of this analysis. More specifically, the mass and width for the η was found to be $m_\eta = 0.545, \sigma_\eta = 0.02883$ (GeV/c^2); and the ϕ mass and width was found to be $m_\phi = 1.02, \sigma_\phi = 0.005917$ (GeV/c^2). Due to the high amount of statistics associated with this topology at this point, it was only necessary to include fifteen files to perform this study.

After the fits for the ϕ and η peaks were performed at different confidence levels, an integration of the Gaussian function and polynomial function was calculated. The results of these integrations plotted as a function of kinematic fit confidence level provides an indication of where an appropriate confidence

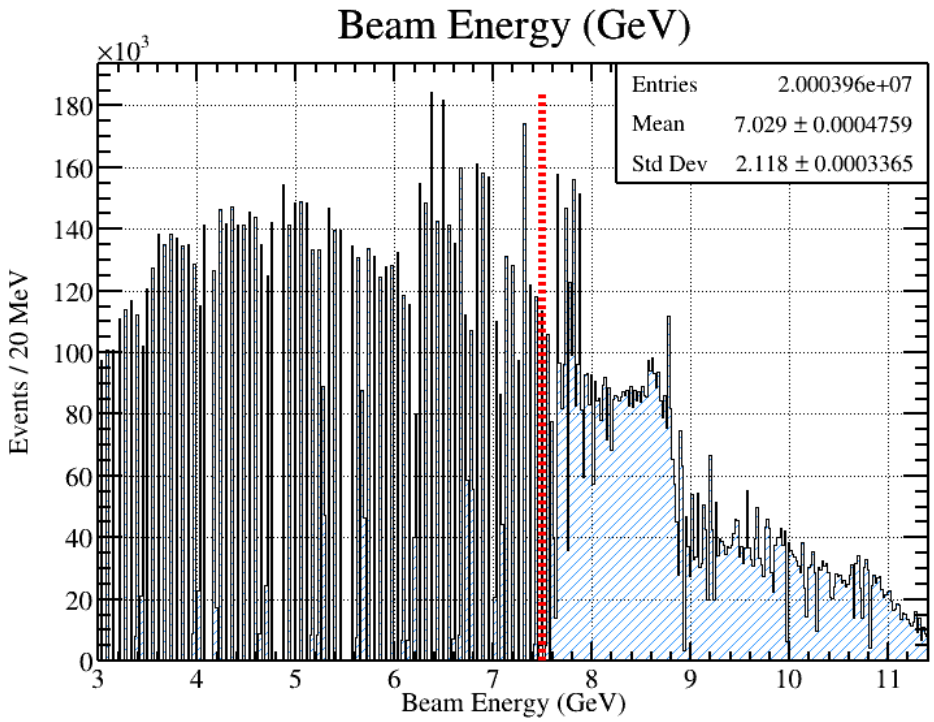

Figure 7: An example histogram of the beam energy distribution at GlueX. One can easily notice the large amount of statistics present around the coherent peak region ($8.0GeV - 8.8GeV$) and energies above it. Also contained in the image is a red dashed line which represents the cut value used on this data to select beam energies above 7.5 GeV.

level cut should be for this analysis. The outcomes of these integrations are provided in Figure 10 for the η meson and also in Figure 11 for the ϕ meson. Both figures contain a red and green line where the red line is the integrated value for the background polynomial and the green line is the integrated value for the Gaussian fit. Each plot contains ten points, denoted with a + symbol, which represent the values obtained at different kinematic fit confidence level values. One can easily observe that for both the ϕ and η plots, the integration of background events drops substantially as the kinematic fit confidence level cut becomes tighter. Additionally, the integration of signal events stays relatively flat as a function of cut value, an indication that the kinematic fitter is performing correctly. Ultimately, the value of $1x10^{-4}$ was chosen as the final kinematic fit cut value since it removed a large amount of background events for both the ϕ and η, while also preserving an appropriate amount of signal events.

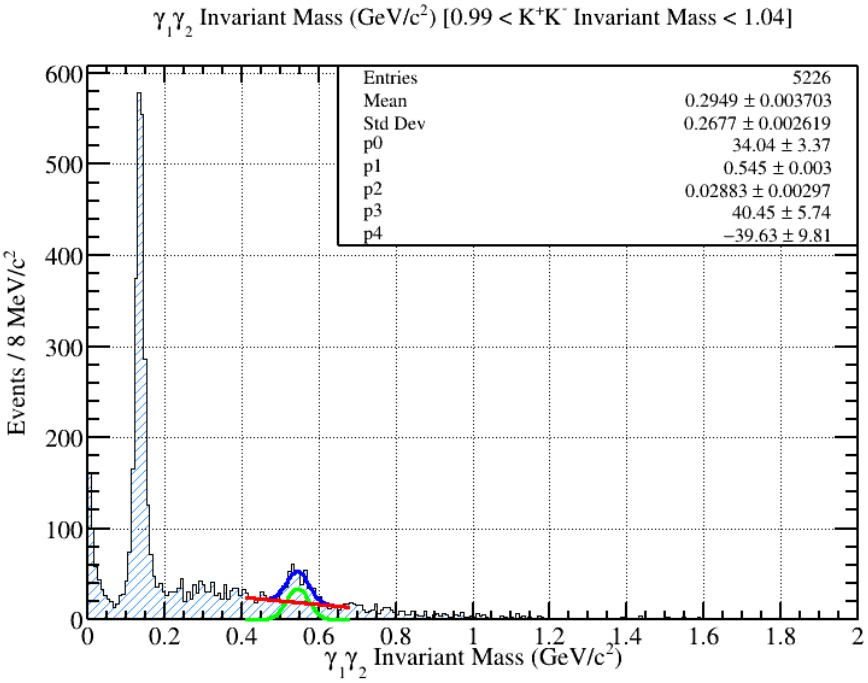

Figure 8: The $\gamma_1\gamma_2$ invariant mass obtained after a kinematic fit confidence level cut of $1x10^{-4}$ and requiring the K^+K^- invariant mass be between the values of 0.99 and 1.04 GeV/c^2 in order to reduce redundant backgrounds. The spectra shows clear π^0 and η peaks at appropriate mass value. The figure also includes three fits where the blue line represents a Gaussian plus a first degree polynomial, the green line represents the Gaussian fit, and the red line represents the first degree polynomial. The constants associated with these fits are listed in the legend.

1.4 Investigation of $\phi\eta$ correlation by means of K^+K^- Vs $\gamma_1\gamma_2$ Invariant Mass Plot

The image illustrated in Figure 12 is the data in question. On the vertical axis is the K^+K^- invariant mass and on the horizontal axis is the $\gamma_1\gamma_2$ invariant mass. To be absolutely clear, this is a plot of invariant mass versus invariant mass and is therefore not a Dalitz Plot. Some interesting features contained within the image are the clear vertical bands for the π^0 and η resonances which have large decay modes to $\gamma\gamma$ final states. In addition, one can also observe a horizontal band slightly above 1 $\frac{GeV}{c^2}$ which corresponds to the ϕ meson decaying to a K^+K^- final state. This analysis will focus on the region where the ϕ meson and η meson bands cross in order to determine if their intersection region contains some type of correlation.

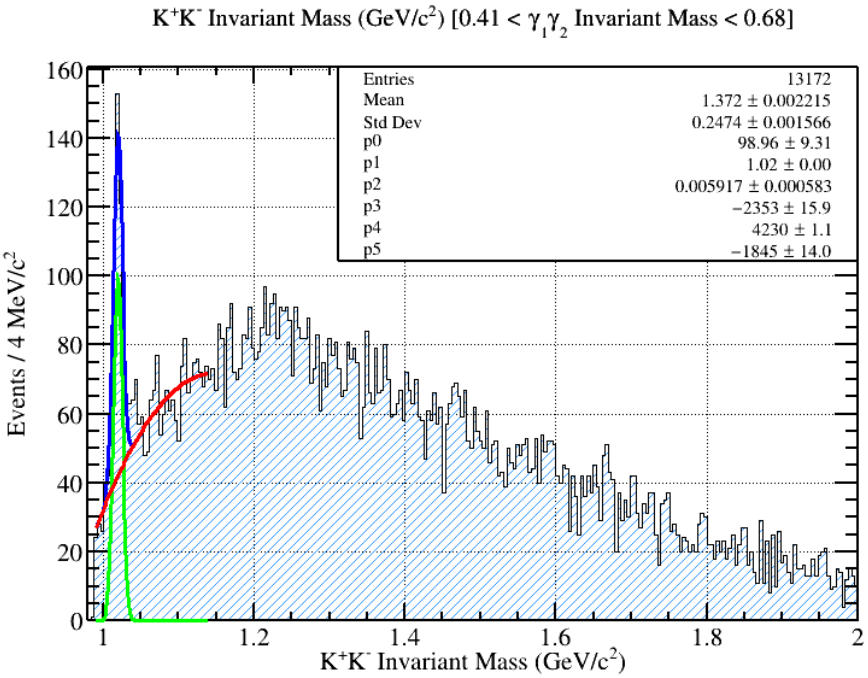

Figure 9: The K^+K^- invariant mass obtained after a kinematic fit confidence level cut of $1x10^{-4}$ and requiring the $\gamma_1\gamma_2$ invariant mass be between the values of 0.41 and 0.68 GeV/c^2 in order to reduce redundant backgrounds. The spectra shows a clear ϕ peak with a minimal amount of background. The figure also includes three fits where the blue line represents a Gaussian plus a second degree polynomial, the green line represents the Gaussian fit, and the red line represents the second degree polynomial. The constants associated with these fits are listed in the legend.

1.4.1 Cuts on the 2D Invariant Mass Plot

In order to analyze the $\phi\eta$ region of this data, only events which fall within $\pm 10\sigma_\phi$ away from the ϕ peak and $\pm 10\sigma_\eta$ away from the η peak will be considered. This was done by taking different slices of either the $\gamma\gamma$ or K^+K^- data, then projecting the invariant mass distribution onto the opposite axis. For example, there were five different ϕ mass regions studied in this analysis. Each fit corresponds to a different $\gamma\gamma$ mass range. The $\gamma\gamma$ mass ranges are all $4\sigma_\eta$ in width, and span a total mass range of $m_\eta - 10\sigma$ to $m_\eta + 10\sigma$. An illustrated example with labeled cut lines is provided in Figure 13. It should be noted that the analysis of the η mass was not studied symmetrically about the ϕ due to the fact that going more than $m_\phi - 6\sigma_\phi$ away from the ϕ peak would result in no events because of the K^+K^- threshold.

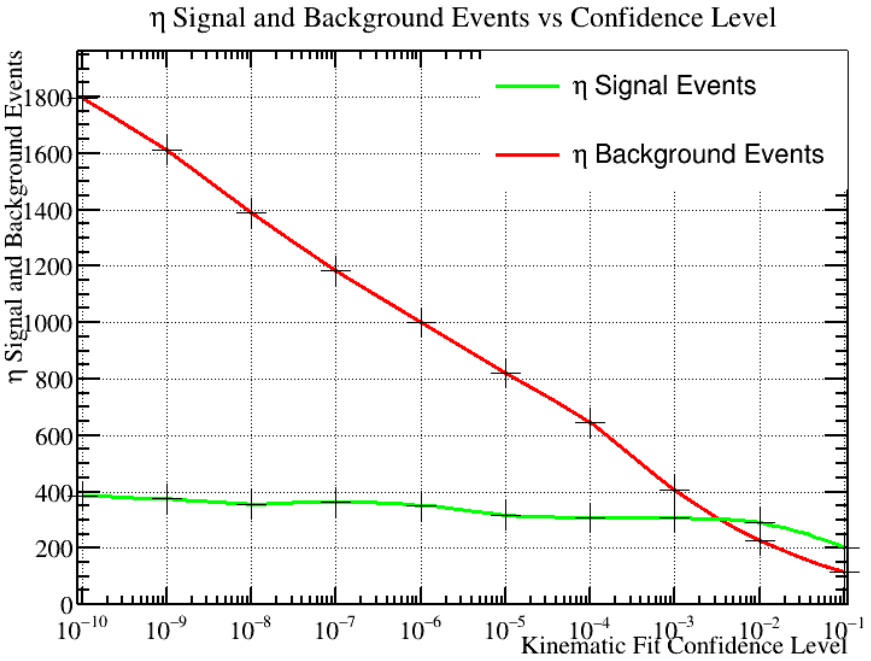

Figure 10: A graph of the η signal and background events as a function of the kinematic fit confidence level cut. The graph contains a red line which represents the integrated η background events from a first order polynomial, and a green line which represents the integrated η signal events from a Gaussian fit function. The graph indicates that the kinematic fitter is working appropriately such that the total number of background events falls as the kinematic fit confidence level cut is increased. Additionally, the total number of signal events stays relatively flat. This graph helps to provide an appropriate kinematic fit cut value that will be used for the rest of this analysis.

1.4.2 Projections and Fits for ϕ and η

Once the data had been cut and projected in the ten different mass regions, the ϕ and η peaks were fit. In the instance of the ϕ meson, the signal plus background events were fit with a Gaussian plus a second degree polynomial. The fit range used in each histogram projection for the ϕ meson spans from $m_\phi - 6\sigma_\phi$ to $m_\phi + 30\sigma_\phi$ $\frac{GeV}{c^2}$. The unusually large fit range was necessary in order to properly estimate the background surrounding the ϕ mass. In the instance of the η meson, the signal plus background events were fit with a Gaussian plus a first degree polynomial due to the relatively flat background surrounding the η peak. The fit range used for the η meson spans $m_\eta \pm 6\sigma_\eta$ $\frac{GeV}{c^2}$. The resulting fits are provided in the images below where the

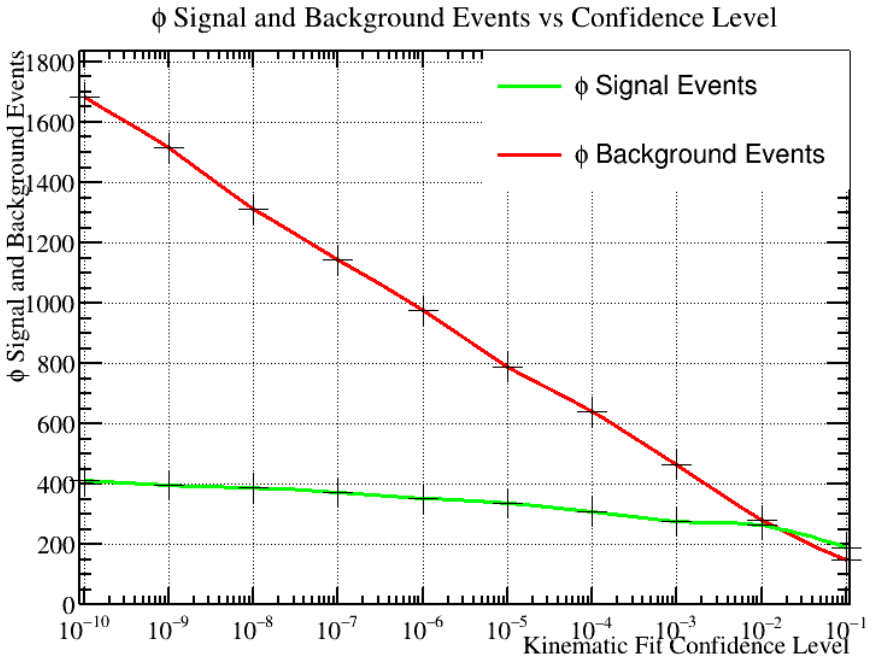

Figure 11: A graph of the ϕ signal and background events as a function of the kinematic fit confidence level cut. The graph contains a red line which represents the integrated ϕ background events from a second order polynomial, and a green line which represents the integrated ϕ signal events from a Gaussian fit function. Just like the η graph before it in Figure 8, the total number of background events falls as the kinematic fit confidence level cut is increased and the total number of signal events stays relatively flat.

blue line represents the fit for all events (signal plus background), the green line represents the Gaussian fit (signal events), and the red line represents the polynomial fit (background events). Each histogram contains a title with brackets at the end. The arguments encapsulated by the brackets is the cut range that was used for that particular projection sample.

1.4.3 Integration Results for ϕ and η

After obtaining accurate fits for all regions, integration of the Gaussian fit functions was performed. Each Gaussian fit was integrated in the range of $m \pm 2\sigma_m$, where m represents either m_ϕ or m_η mass coupled with the addition or subtraction of two standard deviations in each direction. Integration of the Gaussian fits provides an accurate estimate for the number of signal events that exists for that particular sampling of $\gamma\gamma$ Vs K^+K^- phase space.

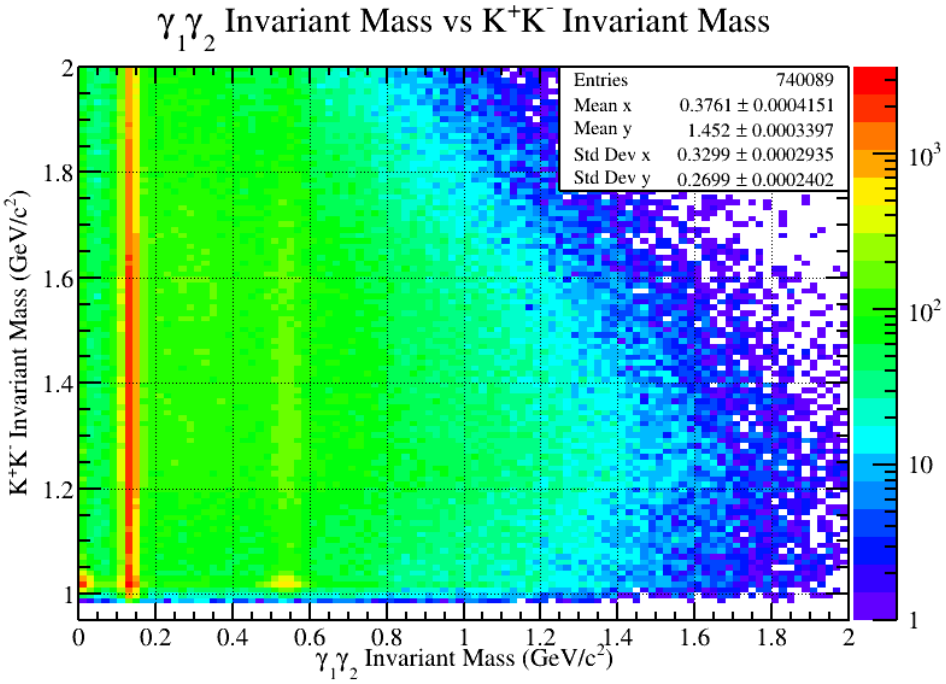

Figure 12: A two dimensional invariant mass plot with the K^+K^- invariant mass on the vertical axis, the $\gamma_1\gamma_2$ invariant mass on the horizontal axis, and a logarithmically scaled z axis. Some interesting features contained within the image are the clear vertical bands for the π^0 and η resonances which have large decay modes to $\gamma\gamma$ final states. In addition, one can also observe a horizontal band slightly above 1 $\frac{GeV}{c^2}$ which corresponds to the ϕ meson decaying to a K^+K^- final state.

The estimated number of signal events have been added to the 2D mass plot below, with the exception of the $\phi\eta$ intersection region which will be discussed in more detail in the Conclusion section.

1.4.4 Additional Statistics Study

In addition to the analysis mentioned above, an additional study has been included which simply samples the phase space and records the number of events within that sample. To do this, the same cut ranges as before were used. The only difference is that only the 3x3 grid surrounding the $\phi\eta$ intersection region. Each region is a box cut which is exactly $4\sigma_\phi$ x $4\sigma_\eta$ in area. Each area is given an index to denote the specific region of phase space that is being sampled and an illustration is provided below.

Using the diagram as a reference, it is easy to see that the average number

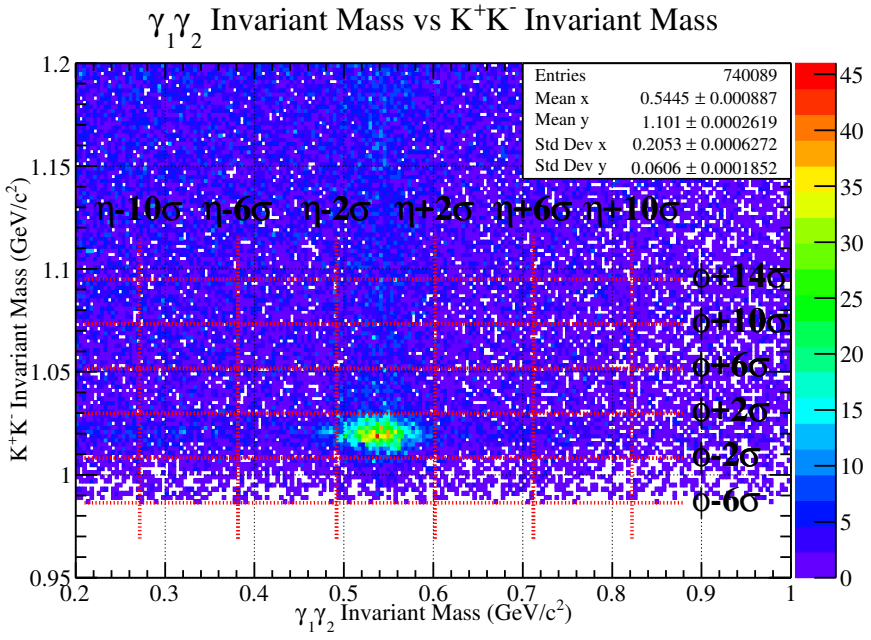

Figure 13: h

of background events within this phase space can be calculated using the formula $N_{BG} = (A_1 + A_3 + A_7 + A_9)/4$. Additionally, the average number of ϕ and η events plus background can be calculated using $N_{BG} + N_\phi = (A_4 + A_6)/2$ and $N_{BG} + N_\eta = (A_2 + A_8)/2$, respectively. Lastly, quantification of the number of correlated events in region 5 is possible by using $N_{BG} + N_\phi + N_\eta + N_{correlated} = A_5$. A figure with the number of events contained within each region of phase space is given below.

The first step of this simplistic analysis is to determine what the average number of background events is, which is calculated to be 453. Knowing this, the number of ϕ and η events can now be determined by using the equations $N_{BG} + N_\phi = (A_4 + A_6)/2$ and $N_{BG} + N_\eta = (A_2 + A_8)/2$, and then subtracting the average number of background events. Upon doing this, it was fount that N_ϕ is 423 and N_η is 433. To complete this analysis, the number of correlated events can now be estimated by using the equation $N_{BG} + N_\phi + N_\eta + N_{correlated} = A_5$, and subtracting N_{BG}, N_ϕ, and N_η. The total number of correlated events is 2446. This calculations shows once again that there is an overflow of events within the $\phi\eta$ intersection region that cannot be explained by the presence of background or the addition of events from

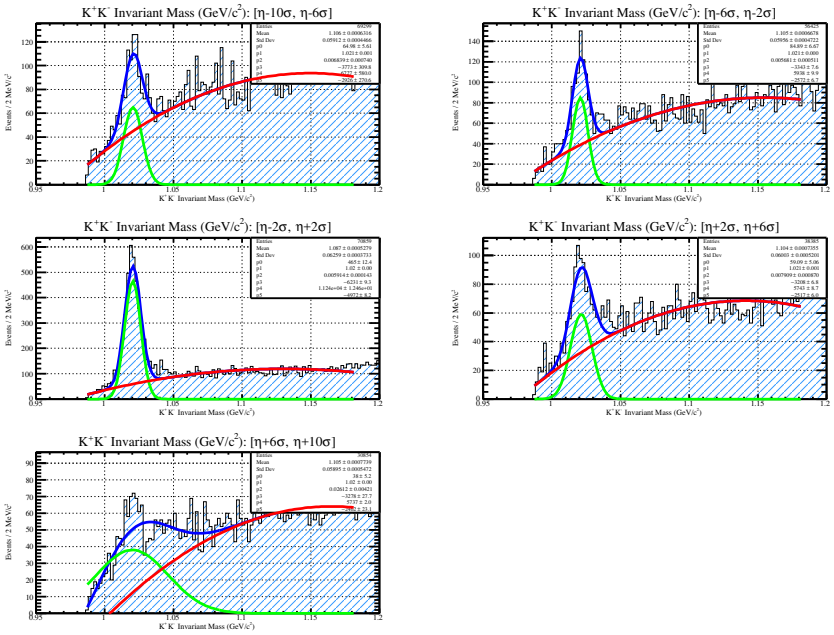

Figure 14: Here

the ϕ and η bands.

1.4.5 Conclusion of K^+K^- Vs $\gamma_1\gamma_2$ Invariant Mass Plot Study

Given that the number of estimated signal events has been calculated for the ϕ and η bands which neighbor the $\phi\eta$ intersection region, the expected number of events will be in the $\phi\eta$ intersection region using averages can be estimated. Taking the numbers from the two dimensional plot above and rounding to the nearest integer, the average number of signal events in the ϕ band is $\overline{\phi_{events}} \sim 482$, and the average number of signal events in the η band is $\overline{\eta_{events}} \sim 500$. Therefore, it is estimated that the number of signal events within the $\phi\eta$ intersection region should be just shy of 1000 events if there is no correlation present. After integrating the Gaussian fit for the ϕ and η mesons in the $\phi\eta$ intersection region, it was found that there were 3194 events corresponding to the ϕ fit, and 2993 events corresponding to the η fit. Both of these fits not only yield roughly the same number of events, but they also produce an event estimate which is a factor of three higher than what would have been there from the ϕ and η bands alone. The large increase in event statistics within the $\phi\eta$ intersection region strongly suggests that some

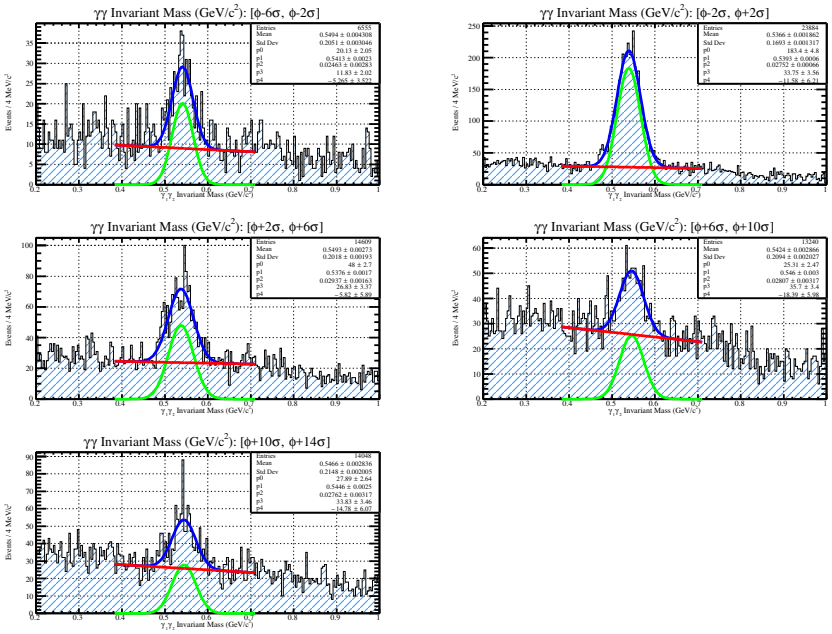

Figure 15: Here

type of correlation is present within this area of K^+K^- $\gamma\gamma$ phase space. It should be clearly noted that the nature of this correlation is not identified at this time. Moreover, it is unclear from this study as to whether or not the bound stats is mesonic or baryonic in nature. Additional studies on this area of phase space need to be performed in order to establish that this spike in statistics is not coming from the $\gamma p \to N^*\phi$, $N^* \to p\eta$ topology.

1.5 Monte Carlo

1.6 Analysis of Beam Asymmetry

1.7 Analysis of $\phi\eta$ Invariant Mass Plot

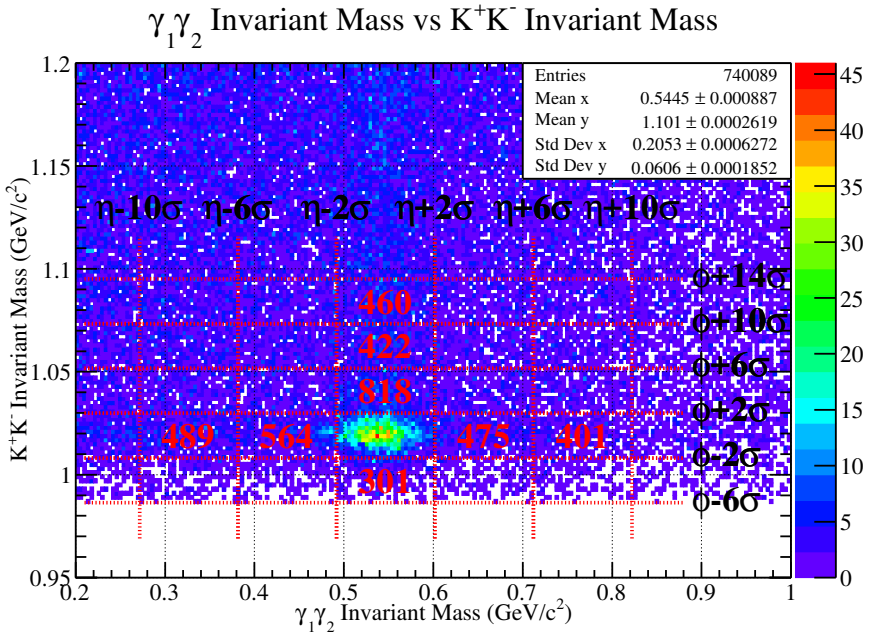

Figure 16: Here

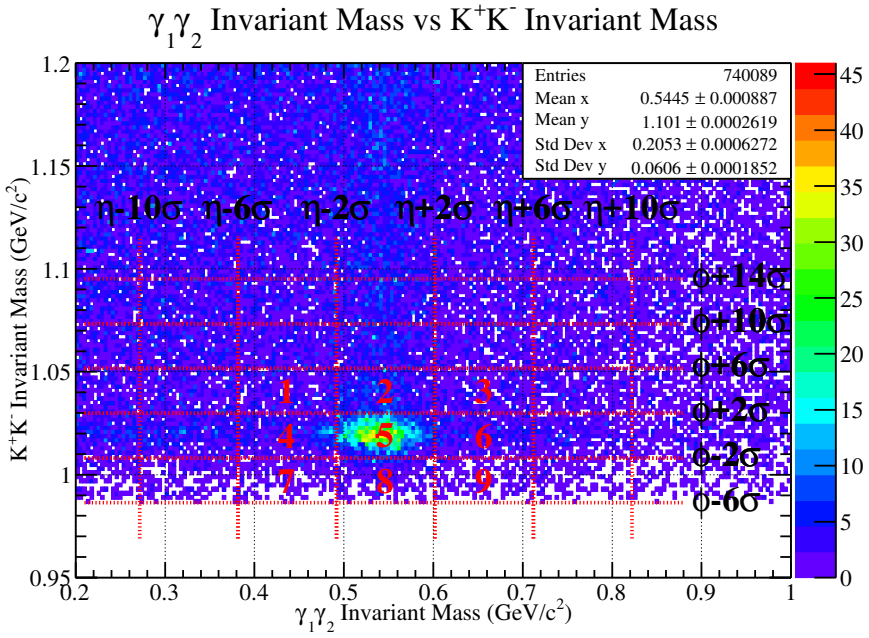

Figure 17: Here

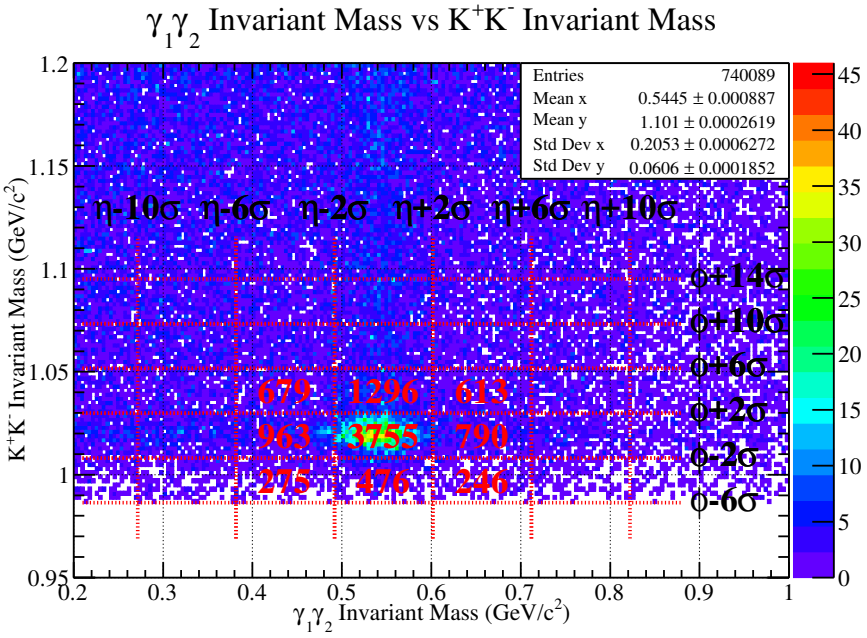

Figure 18: Here